Ultrasound in Med. & Biol., Vol. 37, No. 9, pp. 1478–1485, 2011

0301-5629/$ - see front matter

doi:10.1016/j.ultrasmedbio.2011.05.846

● *Original Contribution*

SONODYNAMIC EFFECT OF AN ANTI-INFLAMMATORY AGENT – EMODIN ON MACROPHAGES

Qianping Gao,*† Fengping Wang,‡ Shuyuan Guo,‡ Jingyi Li,* Bidan Zhu,* Jiali Cheng,‡ Yinghua Jin,‡ Bo Li,‡ Huan Wang,† Sa Shi,* Qiang Gao,§ Zhiguo Zhang,§ Wenwu Cao,§‖ and Ye Tian*‡

*Department of Pathophysiology, Harbin Medical University, Harbin, P. R. China; †The First Affiliated Hospital of Harbin Medical University, Harbin, P. R. China; ‡The Second Affiliated Hospital of Harbin Medical University, Harbin, P. R. China; §Department of Physics, Harbin Institute of Technology, Harbin, P. R. China; and ‖Materials Research Institute, Pennsylvania State University, University Park, PA, USA

(*Received* 20 *November* 2010; *revised* 19 *May* 2011; *in final form* 31 *May* 2011)

Abstract—Emodin has been used as an anti-inflammatory agent and inflammation is a crucial feature of atherosclerosis. Here, we investigated the sonodynamic effect of emodin on macrophages, the pivotal inflammatory cells in atherosclerotic plaque. THP-1 derived macrophages were cultured with emodin and exposed to ultrasound. Six hours later, unlike the cells treated for 5 and 10 min, the viability of cells treated for 15 min decreased significantly and the cells showed typical apoptotic chromatin fragmentation. The percentage of apoptotic and necrotic cells in the sonodynamic therapy (SDT) group was higher than that in the ultrasound group. Two hours after treatment for 15 min, the cytoskeleton lost its original features as the filaments dispersed and the cytoskeletal proteins aggregated. The percentage of cells with disturbed cytoskeletal filaments in the SDT group was higher than that in the ultrasound group. These results suggest emodin has a sonodynamic effect on macrophages and might be used as a novel sonosensitizer for SDT for atherosclerosis. (E-mail: dzk@psu.edu and yetian@ems.hrbmu.edu.cn)

Key Words: **Atherosclerosis, Inflammation, Macrophage, Emodin, Sonodynamic therapy.**

INTRODUCTION

Atherosclerosis (AS) is a complex disease with several possible contributing factors. Inflammation is implicated in the pathogenesis of AS, especially in vulnerable plaque that triggers the onset of acute cardiovascular events (Hermus et al. 2010; Libby and Aikawa 2002). Photodynamic therapy (PDT) could induce the regression of atherosclerotic plaque (Waksman et al. 2008). The mechanism involves the effect of reducing the infiltration of macrophages, which are the metabolically active inflammatory cells in atherosclerotic plaque (Liu and Hamblin 2005). However, the application of PDT is limited to superficial lesions because of its definite penetration. Unlike PDT, sonodynamic therapy (SDT) can penetrate deeply into tissues (Tachibana et al. 2008).

The sonosensitizer is crucial for effective SDT. Most sonosensitizers come from photosensitizers (Wang et al. 2010c; Dai et al. 2009), which makes them liable to cause photodermatitis and they are not generally used in clinical practice. To avoid photodermatitis, developing a new sonosensitizer that can be widely used is necessary. Emodin from rhubarb, a natural herb, is widely used as a laxative and has other versatile biologic properties, such as anti-inflammation, anti-proliferation and anti-carcinoma (Liu et al. 2010; Chen et al. 2009; Lin et al. 2009; Hu et al. 2009; Cai et al. 2008). Emodin was found to stabilize atherosclerotic plaque in fat-fed apolipoprotein E-deficient mice, probably through its anti-inflammatory property (Zhou et al. 2008). Emodin is a naturally occurring and structurally related anthraquinone, which is a well-known photosensitizer (Buytaert et al. 2006). However, whether emodin can induce apoptosis or necrosis of human macrophages under ultrasound exposure is unknown.

Address correspondence to: Ye Tian, Department of Cardiology, The Second Affiliated Hospital of Harbin Medical University; The Key Laboratory of Myocardial Ischemia Mechanism and Treatment, Ministry of Education, Harbin 150086, P. R. China. E-mail: yetian@ems.hrbmu.edu.cn and Wenwu Cao, Materials Research Institute, Pennsylvania State University, University Park, PA 16802 USA. E-mail: dzk@psu.edu

We hypothesized that emodin could induce apoptosis or necrosis of macrophages under ultrasound exposure. In this study, we attempted to combine emodin with low-intensity ultrasound exposure to determine whether emodin can mediate sonodynamic therapy for macrophages.

MATERIALS AND METHODS

Reagents

Emodin was provided by the National Institute for the Control of Pharmaceutical and Biological Products (Beijing, China). The reagent is a commercial product of analytical grade with purity above 98% and it was dissolved in 100% dimethyl sulfoxide (DMSO) and stored at −20°C in the dark. The stock solutions were diluted 10- to 10^3-fold for the experiments. The final concentration of DMSO in cells was less than 0.1%. Roswell Park Memorial Institute (RPMI) medium (1640) and fetal bovine serum were obtained from Hyclone Chemical Co. (Thermofisher Biotechnology, Beijing, China). Benzylpenicillin-streptomycin was obtained from Beyotime Biotechnology (Jiangsu, China). Phorbol-12-myristate-13-acetate (PMA) was obtained from EMD Biosciences, Inc. (La Jolla, CA, USA). Hoechst 33342 and propidium iodide (PI) were purchased from Sigma Chemical Co., Ltd. (Santa Clara, CA, USA). A rabbit polyclonal antibody against vimentin (ab8545) was obtained from Abcam, Ltd. (Hong Kong, China). A rabbit polyclonal antibody against β-tubulin (H-235) and a goat polyclonal antibody against α-actin (C-11) were obtained from Santa Cruz Biotechnology, Inc. (Santa Cruz, CA, USA). All other drugs and chemicals used for this study were purchased from Sigma Chemical Co., Ltd.

Measurements of absorption and fluorescence spectra of emodin

The absorption spectrum of emodin was measured with a spectrophotometer (USB 2000; Ocean Optics Incorporated, Dunedin, FL, USA) under a deuterium lamp and a 40 W wolfram lamp. The fluorescence spectrum of emodin was measured with a spectrophotometer at a wavelength of 405 nm.

Cells culture

THP-1 cells (ATCC, Rockefeller, MD, USA) were cultured in RPMI Medium (1640) supplemented with 10% fetal bovine serum and 50×10^{-3} g/L benzylpenicillin-streptomycin. Cells were maintained at 37°C, with 5% CO_2/95% air in a humidified incubator and they were harvested for passage when they reached confluence. For experiments, cells were seeded in microculture dishes (Costar; Corning Incorporated, Corning, NY, USA) in their usual medium plus PMA at a concentration of 10×10^{-3} g/L for 72 h (Osto et al. 2008; Ning et al. 2009). The medium was removed and replaced with fresh medium without PMA.

Detection of intracellular uptake of emodin

Cells were seeded in 35-mm Petri dishes with 1×10^4 cells/mL. Emodin was added at a final concentration of 15×10^{-3} g/L. After 2 h, the cells were washed twice with phosphate buffered saline (PBS) and the uptake of emodin by the cells was examined with a fluorescence microscope (IX71; Olympus, Tokyo, Japan) using a filter with an excitation wavelength of 420–480 nm and an emission wavelength of 480–550 nm.

Ultrasound exposure system

The ultrasound exposure system **is** shown in Figure 1 (838A-H-O-S ultrasonic device; Sheng Xiang Technology, Shenzhen, China). The ultrasound transducer, with a diameter of 38 mm, was submerged in a container filled with degassed water. The overall resonant frequency of the transducer was 0.86 MHz. The reading output power intensity from the amplifier was 2 W/cm^2. The target depth of the ultrasound was 10 cm below the transducer surface. The output acoustic pressure was measured in degassed water 10 cm from the transducer surface. The output intensity was 0.44 W/cm^2. For all experiments, degassed water was used as the ultrasonic medium. The solution inside the Petri dishes was buffered from overheating by the water around the Petri dishes, and the temperature was set to room temperature (23–25°C). During the sonication procedure, the temperature of the solution inside the Petri dishes did not rise more than 0.1°C, as measured with a thermometer.

Sonodynamic therapy

MTT assay. Cells (1×10^5 cells/mL) were seeded in 35-mm Petri dishes. Cells were incubated with emodin at a concentration of 15×10^{-3} g/L for 2 h in the dark. They were then exposed to pulse ultrasound for 5–15 min. Control Petri dishes were sham-exposed to ultrasound. After SDT, each Petri dish was incubated for 6 h before

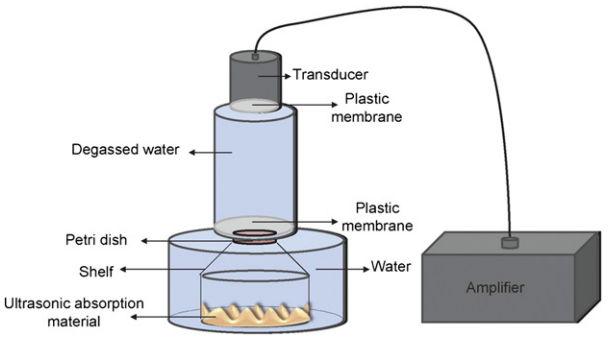

Fig. 1. The ultrasound exposure system.

the MTT assay was performed. Mitochondrial function was expressed as a percentage of viable treated cells relative to untreated control cells (without ultrasound and drug). All experiments were repeated three times independently.

Hoechst PI. Petri dishes were seeded with 1×10^4 cells/mL. The SDT experiments included an emodin concentration of 15×10^{-3} g/L and ultrasound exposure for 15 min. Six hours later, the cell monolayer was stained with Hoechst-PI nuclear dye. The cell monolayer was washed twice with PBS, then examined under a fluorescence microscope using a filter with an excitation wavelength of 330–385 nm and an emission wavelength of 420–480 nm. The percentages of apoptotic and necrotic cells were calculated from the total cell numbers (total cells = alive + apoptotic + necrotic cells). All cells from 10 random microscopic fields at ×40 magnification were counted. Experiments were repeated three times independently.

Immunofluorescence staining. The SDT experiments included an emodin concentration of 15×10^{-3} g/L and ultrasound exposure for 15 min. Two hours after SDT, the cells were fixed with paraformaldehyde (PFA). The cells were perforated with a detergent such as Triton X-100 to allow exposure of the antibodies to the structures inside the cells. To avoid non-specific binding of the second antibody, the cells were blocked with 1% BSA at room temperature for 1 h. Primary antibodies were added at 37°C for 1 h. Then, the secondary antibody, which was conjugated with fluorescein isothiocyanate (FITC), was added at 37°C for 2 h. 4',6-diamidino-2-phenylindole (DAPI) was added at room temperature for 2 min. The cell monolayer was washed twice with PBS and then examined under a fluorescence microscope using a filter with an excitation wavelength of 330–385 nm and an emission wavelength of 420–480 nm and one with an excitation wavelength of 420–480 nm and an emission wavelength of 480–550 nm. The status of cytoskeletal protein polymerization was calculated by randomly choosing at least 10 microscopic fields at ×40 and counting cells in the field as either having cytoskeletal filaments that were intact or disturbed. The percentage of cells with disturbed protein filaments was expressed as the number of cells with disturbed cytoskeletal filaments/the total number of cells.

Statistical analysis

All values were expressed as the means ± standard deviation. Dunnett-T and SNK tests were used to assess the effects of various emodin concentrations on cell viability without ultrasound exposure. The LSD and SNK tests were used to assess the effects of sonoactivated emodin on cell viability: p values < 0.05 were considered significant.

RESULTS

Figure 2 shows the structure, absorption spectrum and emission spectrum of emodin. Panel A: the structure of emodin; panel B: the absorption spectrum of emodin under a wolfram lamp; panel C: the fluorescence

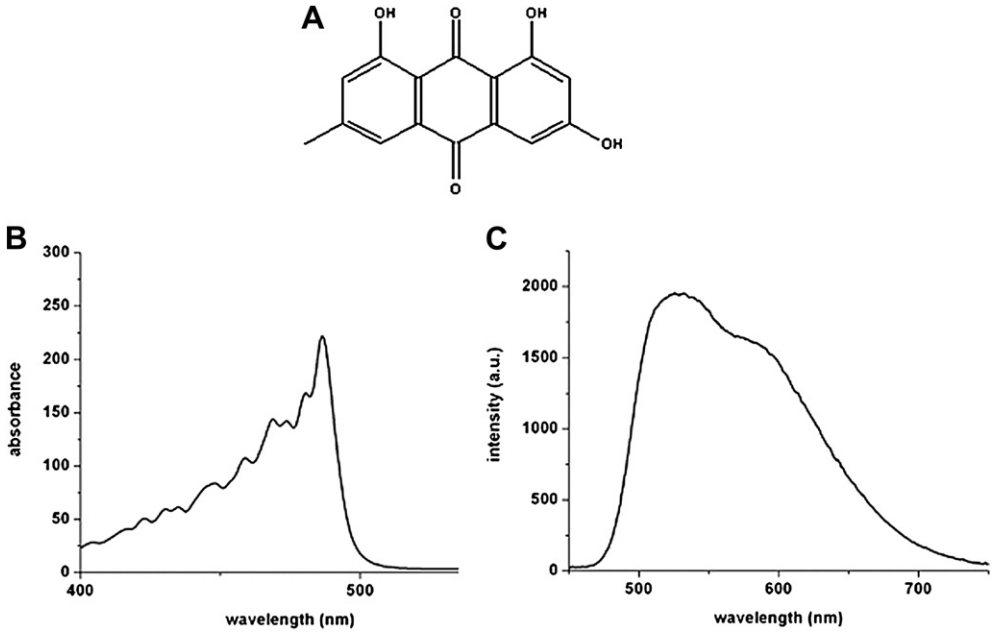

Fig. 2. The structure and spectrum of emodin. Panel A: the structure of emodin; panel B: the absorption spectrum of emodin under a wolfram lamp; panel C: the fluorescence emission spectrum of emodin at 405 nm.

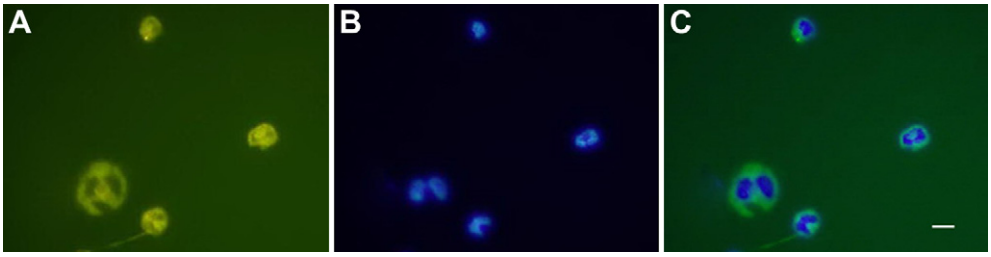

Fig. 3. The intracellular accumulation of emodin (×200). Panel A: emodin fluorescence in unfixed macrophages; panel B: nuclei of the same cells after staining with Hoechst 33342 nuclear dye; panel C: a merged image of A and B. Scale bar: 20 μm.

emission spectrum of emodin at 405 nm. The data show that the absorption wavelength of emodin is less than 500 nm
and the fluorescence emission wavelengths of emodin range from 480 nm to 700 nm.

Figure 3 shows the distribution of emodin inside macrophages. Panel A: emodin fluorescence in unfixed macrophages; panel B: nuclei of the same cells after staining with Hoechst 33342 nuclear dye; panel C: a merged image of A and B. Emodin appears to be distributed in cytoplasm.

As shown in Figure 4, cell viability decreased significantly from 90 ± 9% (10 min) to 54 ± 5% (15 min) in cells treated with emodin-SDT. Cell viability decreased from 93 ± 5% (10 min) to 72 ± 9% (15 min) in cells treated with ultrasound alone. Cell viability decreased more significantly in cells treated with emodin-SDT for 15 min than ultrasound alone (54 ± 5% vs. 72 ± 9%, $P < 0.01$). Cell viability was not significantly affected in cells treated for 5 min and 10 min ($p > 0.05$). Treatment with emodin alone did not affect cell viability compared with the control ($p > 0.05$). DMSO at a concentration of 0.1% showed no effect on cell viability under ultrasound (data not shown).

Figure 5 shows the apoptosis and necrosis of cells 6 h after emodin-SDT. The controls and cells treated with emodin alone showed uniform blue fluorescence (Fig. 5A1 and A2); apoptotic cells were seen as bright

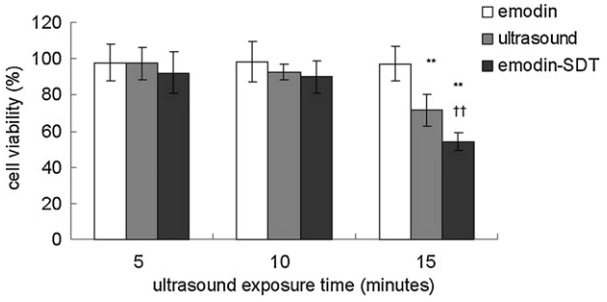

Fig. 4. Cell viability after emodin-sonodynamic therapy (SDT) assessed by MTT assay. The results show that cell viability decreased with increasing ultrasound exposure time. $^{**}p < 0.01$ vs. the control; $^{\dagger\dagger}p < 0.01$ vs. ultrasound alone.

blue fluorescence spots and necrotic nuclei were identified by the presence of staining with PI, which was evident as pink fluorescence (Fig. 5A3 and A4). The percentages of apoptotic cells in the ultrasound group and the SDT group were higher than that of the control (26 ± 6% vs. 4 ± 3%, $p < 0.01$; 32 ± 6% vs. 4 ± 3%, $p < 0.01$, respectively). The percentage of apoptotic cells in the SDT group was higher than that in the ultrasound group (32 ± 6% vs. 26 ± 6%, $p < 0.05$.). The percentages of necrotic cells in the ultrasound group and the SDT group were higher than that of the control (5 ± 2% vs. 2 ± 1%, $p < 0.05$; 17 ± 5% vs. 2 ± 1%, $P < 0.01$, respectively). The percentage of necrotic cells in the SDT group was higher than that in the ultrasound group (17 ± 5% vs. 5 ± 2%, $p < 0.01$). There was no discernible difference in the percentage of apoptotic and necrotic cells between the emodin treated group and the controls.

Figure 6 shows morphologic changes of the cytoskeleton 2 h after emodin-SDT. Cells were fixed and incubated with α-actin, β-tubulin and vimentin antibodies to stain cytoskeletal protein (green fluorescence) and with DAPI to stain nuclei (blue fluorescence). Control cells showed a regular cytoskeletal network seen as green fluorescence, and nuclei showed uniform blue fluorescence (Fig. 6A-a1, b1 and c1). There were no obvious morphologic changes of the cytoskeleton in cells treated with emodin alone (Fig. 6A-a2, b2 and c2). The fluorescence signal of cytoskeletal protein was slightly attenuated 2 h after ultrasound exposure in some cells, as shown in Figure 6A-a3, b3 and c3 (indicated with arrowheads). In the case of cells treated with emodin-SDT, α-actin, β-tubulin and vimentin filaments dispersed and the proteins aggregated. The cytoskeleton lost its original features, as shown in Figure 6A-a4, b4 and c4 (indicated with arrows). The percentages of cells with disturbed cytoskeletal filaments in the ultrasound group and the SDT group were higher than that in the control (α-actin: 29 ± 5% vs. 3 ± 2%, $p < 0.01$; 45 ± 4% vs. 3 ± 2%, $p < 0.01$. β-tubulin: 29 ± 5% vs. 3 ± 2%, $p < 0.01$; 43 ± 9% vs. 3 ± 2%, $p < 0.01$. Vimentin: 29 ± 8% vs. 3 ± 1%, $P < 0.01$; 45 ± 7% vs. 3 ± 1%, $p < 0.01$, respectively). The percentage of cells with disturbed cytoskeletal filaments

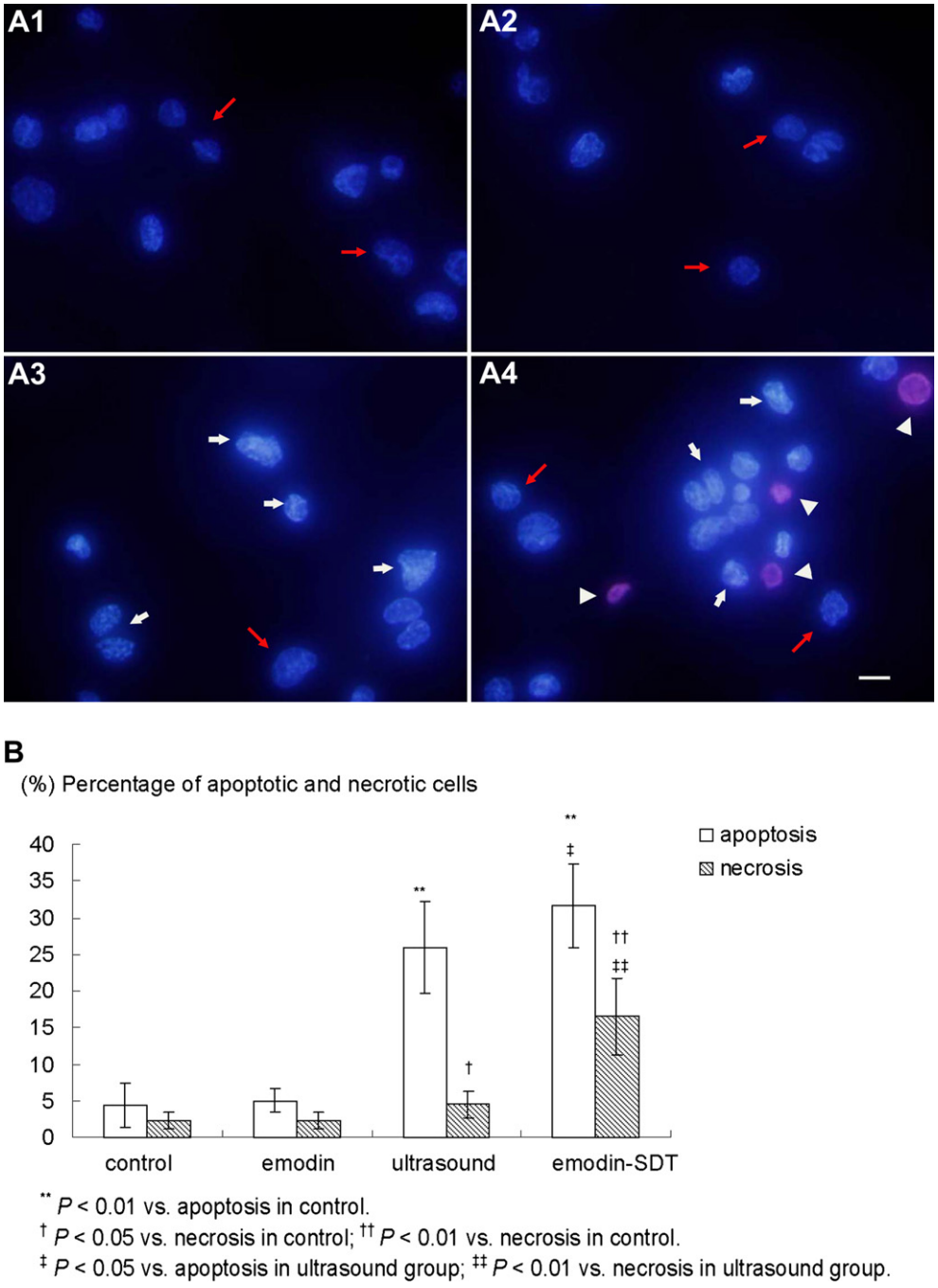

Fig. 5. Apoptosis and necrosis of macrophages induced by emodin-sonodynamic therapy (SDT) (×400). Panel A1: control; panel A2: emodin alone; panel A3: ultrasound alone; panel A4: emodin-SDT. Scale bar: 20 μm. Normal cells are indicated with red arrows. Apoptotic cells are indicated with white arrows. Necrotic nuclei are indicated with arrowheads. Panel B: the percentage of apoptotic and necrotic macrophages 6 h after SDT detected by staining with Hoechst-PI. $^{**}p < 0.01$ vs. apoptosis in the control. $^{\dagger}p < 0.05$ vs. necrosis in the control; $^{\dagger\dagger}p < 0.01$ vs. necrosis in the control. $^{\ddagger}p < 0.05$ vs. apoptosis in the ultrasound group; $^{\ddagger\ddagger}p < 0.01$ vs. necrosis in the ultrasound group.

in the SDT group was higher than that in the ultrasound group (α-actin: 45 ± 4% vs. 29 ± 5%, $p < 0.01$; β-tubulin: 43 ± 9% vs. 29 ± 5%, $p < 0.01$; vimentin: 45 ± 7% vs. 29 ± 8%, $p < 0.01$). There was no difference between the emodin treated group and the controls.

DISCUSSION

SDT is based on energy transition to generate reactive oxygen species (ROS) (Rosenthal et al. 2004), which promote damage to biologic molecules including lipids,

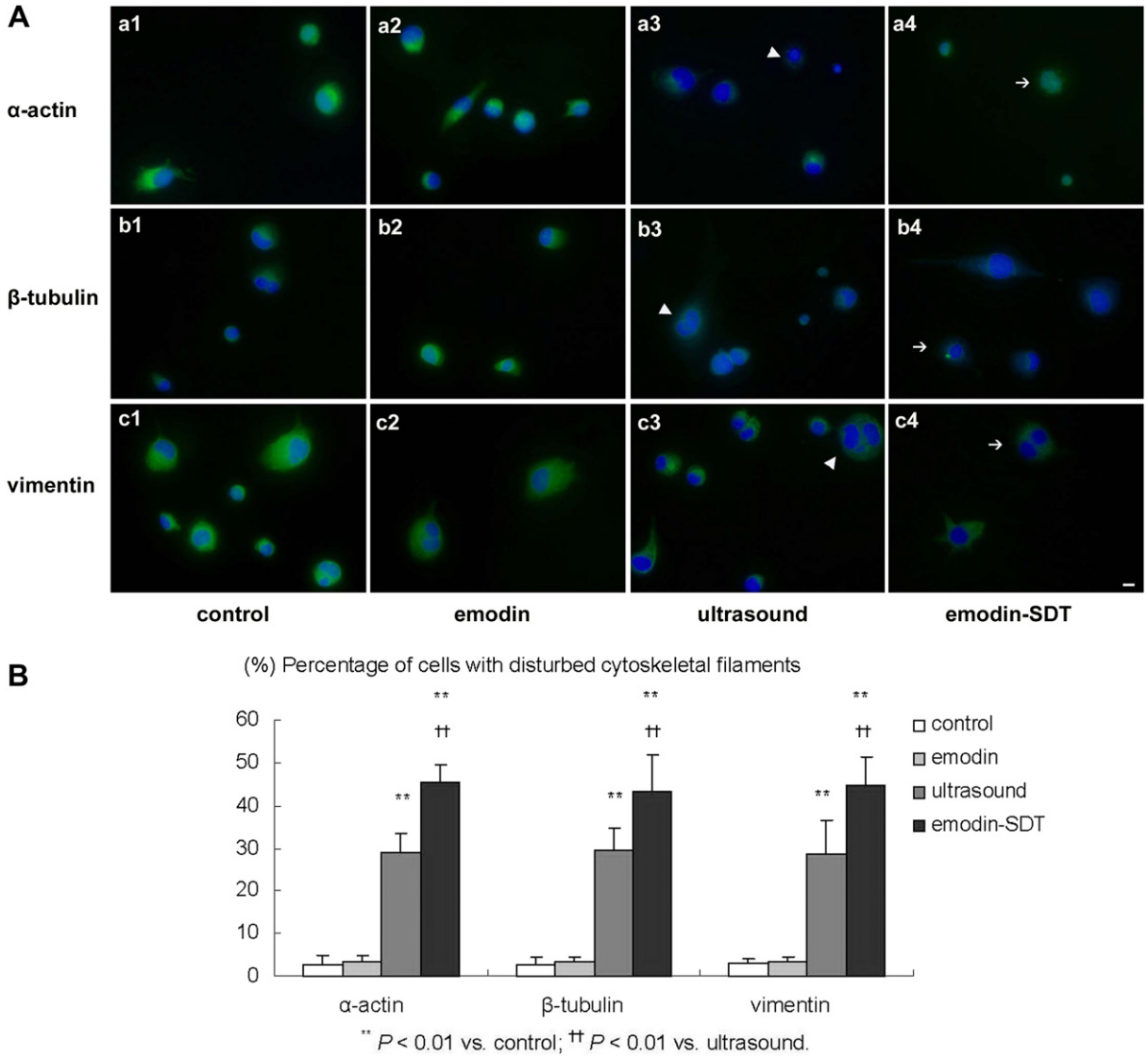

Fig. 6. Morphologic changes of the cytoskeleton induced by emodin-sonodynamic therapy (SDT) (×400). Controls and the cells treated with emodin alone are shown in a1, b1 and c1, and a2, b2 and c2. The cells treated with ultrasound alone are shown in a3, b3 and c3. The cells treated with emodin-SDT are shown in a4, b4 and c4. Scale bar: 20 μm. Panel B: percentage of cells with disturbed cytoskeletal filaments. $^{**}p < 0.01$ vs. the control, $^{\dagger\dagger}p < 0.01$ vs. the ultrasound group.

proteins and DNA. Conjugated macro-π bonds are required to accomplish this energy transition. The more conjugated macro-π bonds inside sensitizer structures, the longer the absorption wavelength of the sensitizers. The number of macro-π bonds inside emodin (Fig. 2A) is less than that of hematoporphyrin and its derivatives (HPDs), so the absorption wavelength of emodin is shorter than that of HPDs. Through measurement of the absorption spectrum, it was shown that emodin absorbed light at wavelengths less than 500 nm (Fig. 2 B and C), shorter than the optical window, that is to say, the minimum in the wavelength region 600–1000 nm enough to fulfill penetration into tissues. To resolve the issue of tissue penetration, ultrasound was used to activate emodin.

During SDT to atherosclerosis, the accumulation of the sonosensitizers at the atherosclerotic lesion is important. The sensitizer targets and accumulates in metabolically active inflammatory cells such as macrophages in the atherosclerotic plaque (Kereiakes et al. 2003; Bialy et al. 2003). In this study, the uptake of emodin by macrophages was detected. The accumulation of emodin in macrophages increased with concentration; however, drug cytotoxicity became obvious gradually along with the increase in concentration (data not shown). Therefore, the definition of a proper drug concentration is necessary. The results indicated that emodin concentration over 20×10^{-3} g/L would kill cells but emodin concentrations below 5×10^{-3} g/L

did not exhibit intracellular drug fluorescence (data not shown). Through detection of emodin fluorescence and the same cell nuclei stained with Hoechst 33342, it was shown that emodin was distributed in the cytoplasm (Fig. 3). Liposoluble sensitizers likely enter cells through LDL-R (Kereiakes et al. 2003; Bialy et al. 2003) and because emodin is liposoluble, it probably enters the macrophages through this receptor and then translocates to the mitochondria to produce a marked effect.

Notable cell death was observed after emodin-SDT. Cell viability decreased gradually as the amount of ultrasound exposure increased. The cell survival rate in the emodin-SDT group was much lower than that in the ultrasound only group under the same exposure conditions (Fig. 4). The results indicated that emodin- SDT could effectively kill macrophages *in vitro*. Moreover, cell viability in the emodin-SDT group was not altered when cells contained only intracellular emodin (data not shown). Cell viability measured by MTT assay reflected dysfunction of the mitochondria. Mitochondrial dysfunction may result from the damage to the mitochondrial structure induced by SDT (Dai et al. 2009; Wang et al. 2010b).

The mode of cell death by PDT and SDT may be either apoptosis or necrosis (Moor 2000). The MTT assay provided some information concerning the function of mitochondria; it did not assess the late, irreversible changes that would indicate the mode of cell death. The Hoechst-PI assay repaired that deficiency. The nuclei of live cells presented uniform blue fluorescence because of resistance to the fluorescence dye (Fig. 5A1 and A2). Apoptotic nuclei presented bright blue fluorescent spots accompanied by nuclear deformation while necrotic nuclei presented pink fluorescence (Fig. 5A3 and A4). In this study, ultrasound exposure alone could induce cell death, which became obvious when the amount of sonication was augmented. This effect was highly enhanced when emodin was added to the cells. The percentage of both apoptotic and necrotic cells increased. There was a synergistic relationship between emodin and ultrasound. Therefore, emodin may be a promising natural sonosensitizer when used at the proper concentration and combined with the appropriate amount of sonication. Hematoporphyrin-SDT induced apoptosis of tumor cells through a mechanism that involved the mitochondria-caspase signaling pathway (Dai et al. 2009; Tang et al. 2010). The mechanism of macrophage apoptosis induced by emodin-SDT may also involve activation of the mitochondria-caspase signaling pathway.

Oxidative stress induced by PDT and SDT can affect several types of biomacromolecules including proteins, lipids and DNA (Davies 2003). In a number of papers, deleterious effects of PDT on the cytoskeleton have been documented (Sakharov et al. 2003; Panzarini et al. 2009; Jung et al. 2009; Casas et al. 2008). By a similar mechanism, SDT can also affect cytoskeletal proteins. Some papers showed that cytoskeleton might represent an important target for SDT (Zhao et al. 2009; Wang et al. 2010a). Cytoplasm skeletal proteins mainly consist of microfilaments, microtubules and intermediate filaments. Vimentin is a kind of middle fiber existing in cells. Its cleavage happens during early apoptosis. In this article, α-actin, β-tubulin and vimentin were observed. The fluorescence signal of cytoskeletal proteins in the cells treated with ultrasound alone was partially attenuated and this attenuation was greatly enhanced by adding emodin. Cytoskeletal filaments were cleaved and formed clusters. The cytoskeleton deformed. No obvious deformation of the cytoskeleton was observed in controls or in cells treated with emodin alone (Fig. 6). It is possible that the disruption of the cytoskeleton is one of the causes of cell death induced by emodin-SDT.

Currently, many possible sonosensitizers have been investigated but few have been approved for clinical use. Rhubarb has been widely used in folk medicine. Emodin, from rhubarb, demonstrates many pharmacologic properties such as regulating cell proliferation and inflammatory cytokines. Moreover, emodin injection has been used in the clinical treatment of viral hepatitis. Emodin promotes atherosclerotic plaque stability *in vivo* (Zhou et al. 2008). The combination of emodin and ultrasound may further stabilize or reduce the atherosclerotic plaque. Therefore, emodin-SDT may be a useful and promising treatment for atherosclerosis. Whether emodin-SDT can induce atherosclerotic plague regression will require further study in animal models.

CONCLUSIONS

Emodin induces the apoptosis and necrosis of macrophages under ultrasound exposure. The results imply emodin-SDT might be a potential treatment for atherosclerosis by reducing the infiltration of macrophages in atherosclerotic plaque.

Acknowledgments—This work was supported by the National Natural Science Foundation of China (30470473; 30970786) and the National 863 Program of China (2007AA02Z450). This work was also supported by the Doctoral Fund of the Ministry of Education of China (20070226026).

REFERENCES

Bialy D, Derkacz A, Wawrzynska M, Bednarkiewicz A, Ziolkowski P, Nowosad H, Strek W. *In vitro* photodynamic diagnosis of atherosclerotic wall changes with the use of mono-l-aspartyl chlorin e6. A preliminary report. Kardiol Pol 2003;59:293–301.

Buytaert E, Callewaert G, Hendrickx N, Scorrano L, Hartmann D, Missiaen L, Vandenheede JR, Heirman I, Grooten J, Agostinis P. Role of endoplasmic reticulum depletion and multidomain

proapoptotic BAX and BAK proteins in shaping cell death after hypericin-mediated photodynamic therapy. FASEB J 2006;20: 756–758.

Cai J, Razzak A, Hering J, Saed A, Babcock TA, Helton S, Espat NJ. Feasibility evaluation of emodin (rhubarb extract) as an inhibitor of pancreatic cancer cell proliferation *in vitro*. JPEN J Parenter Enteral Nutr 2008;32:190–196.

Casas A, Sanz-Rodriguez F, Di Venosa G, Rodriguez L, Mamone L, Blazquez A, Jaen P, Batlle A, Stockert JC, Juarranz A. Disorganization of cytoskeleton in cells resistant to photodynamic treatment with decreased metastatic phenotype. Cancer Lett 2008;270:56–65.

Chen GL, Liu ZY, Wang J, Gao X, Wei LW, Liu YL. Protective effect of emodin against lipopolysaccharides-induced corneal injury in rats. Chin Med Sci J 2009;24:236–240.

Dai S, Hu S, Wu C. Apoptotic effect of sonodynamic therapy mediated by hematoporphyrin monomethyl ether on C6 glioma cells *in vitro*. Acta Neurochir (Wien) 2009;151:1655–1661.

Davies MJ. Singlet oxygen-mediated damage to proteins and its consequences. Biochem Biophys Res Commun 2003;305:761–770.

Hermus L, Lefrandt JD, Tio RA, Breek JC, Zeebregts CJ. Carotid plaque formation and serum biomarkers. Atherosclerosis 2010;213:21–29.

Hu Q, Noor M, Wong YF, Hylands PJ, Simmonds MS, Xu Q, Jiang D, Hendry BM, Xu Q. *In vitro* anti-fibrotic activities of herbal compounds and herbs. Nephrol Dial Transplant 2009;24:3033–3041.

Jung SH, Park JY, Yoo JO, Shin I, Kim YM, Ha KS. Identification and ultrastructural imaging of photodynamic therapy-induced microfilaments by atomic force microscopy. Ultramicroscopy 2009;109: 1428–1434.

Kereiakes DJ, Szyniszewski AM, Wahr D, Herrmann HC, Simon DI, Rogers C, Kramer P, Shear W, Yeung AC, Shunk KA, Chou TM, Popma J, Fitzgerald P, Carroll TE, Forer D, Adelman DC. Phase I drug and light dose-escalation trial of motexa-fin lutetium and far red light activation (phototherapy) in subjects with coronary artery disease undergoing percutaneous coronary intervention and stent deployment procedural and long-term results. Circulation 2003; 108:1310–1315.

Libby P, Aikawa M. Stabilization of atherosclerotic plaques: new mechanisms and clinical targets. Nat Med 2002;8:1257–1262.

Liu Q, Hamblin MR. Macrophage-targeted photodynamic therapy: scavenger receptor expression and activation state. Int J Immunopathol Pharmacol 2005;18:391–402.

Liu T, Jin H, Sun QR, Xu JH, Hu HT. Neuroprotective effects of emodin in rat cortical neurons against beta-amyloid-induced neurotoxicity. Brain Res 2010;1347:149–160.

Lin SY, Lai WW, Ho CC, Yu FS, Chen GW, Yang JS, Liu KC, Lin ML, Wu PP, Fan MJ, Chung JG. Emodin induces apoptosis of human tongue squamous cancer SCC-4 cells through reactive oxygen species and mitochondria-dependent pathways. Anticancer Res 2009;29:327–335.

Moor AC. Signaling pathways in cell death and survival after photodynamic therapy. J Photochem Photobiol B 2000;57:1–13.

Ning Y, Bai Q, Lu H, Li X, Pandak WM, Zhao F, Chen S, Ren S, Yin L. Overexpression of mitochondrial cholesterol delivery protein, StAR, decreases intracellular lipids and inflammatory factors secretion in macrophages. Atherosclerosis 2009;204:114–120.

Osto E, Kouroedov A, Mocharla P, Akhmedov A, Besler C, Rohrer L, von ckardstein A, Iliceto S, Volpe M, Lüscher TF, Cosentino F. Inhibition of protein kinase Cβ prevents foam cell formation by reducing scavenger receptor A expression in human macrophages. Circulation 2008;118:2174–2182.

Panzarini E, Tenuzzo B, Dini L. Photodynamic therapy-induced apoptosis of HeLa cells. Ann N Y Acad Sci 2009;1171:617–626.

Rosenthal I, Sostaric JZ, Riesz P. Sonodynamic therapy–A review of the synergistic effects of drugs and ultrasound. Ultrason Sonochem 2004;11:349–363.

Sakharov DV, Bunschoten A, van Weelden H, Wirtz KW. Photodynamic treatment and H_2O_2-induced oxidative stress result in different patterns of cellular protein oxidation. Eur J Biochem 2003;270: 4859–4865.

Tachibana K, Feril LB Jr, Ikeda-Dantsuji Y. Sonodynamic therapy. Ultrasonics 2008;48:253–259.

Tang W, Liu Q, Zhang J, Cao B, Zhao P, Qin X. *In vitro* activation of mitochondria-caspase signaling pathway in sonodynamic therapy-induced apoptosis in sarcoma 180 cells. Ultrasonics 2010;50: 567–576.

Waksman R, McEwan PE, Moore TI, Pakala R, Kolodgie FD, Hellinga DG, Seabron RC, Rychnovsky SJ, Vasek J, Scott RW, Virmani R. Photo-point photodynamic therapy promotes stabilization of atherosclerotic plaques and inhibits plaque progression. J Am Coll Cardiol 2008;52:1024–1032.

Wang P, Wang X, Liu Q, Zhao X, Cao B, Zhao P. Comparison between sonodynamic effects with protoporphyrin IX and hematoporphyrin on the cytoskeleton of Ehrlich ascites carcinoma cells. Cancer Biother Radiopharm 2010a;25:55–64.

Wang P, Xu C, Xia X, Xu J, Wang X, Xiang J, Leung AW. Mitochondrial damage in nasopharyngeal carcinoma cells induced by ultrasound radiation in the presence of hypocrellin B. J Ultrasound Med 2010b;29:43–50.

Wang XB, Liu QH, Mi N, Wang P, Tang W, Zhao XH, Li XJ. Sonodynamically induced apoptosis by protoporphyrin IX on hepatoma-22 cells *in vitro*. Ultrasound Med Biol 2010c;36:667–676.

Zhao X, Liu Q, Tang W, Wang X, Wang P, Gong L, Wang Y. Damage effects of protoporphyrin IX–Sonodynamic therapy on the cytoskeletal F-actin of Ehrlich ascites carcinoma cells. Ultrason Sonochem 2009;16:50–56.

Zhou M, Xu H, Pan L, Wen J, Guo Y, Chen K. Emodin promotes atherosclerotic plaque stability in fat-fed apolipoprotein E-deficient mice. Tohoku J Exp Med 2008;215:61–69.